RESEARCH ARTICLE

Preparation and Characterization of Silica Coated Magnetic Cu Based MOF as a Nanocarrier for Gradual Release of the Capecitabine Anticancer Drug

Azar Asgari Pari[1], Susan Samadi[2], Mohammad Reza Allahgholi Ghasri[1],Maryam Bikhof Torbati[2], Mohammad Yousefi[3]*

[1]Department of Chemistry, Yadegar-e Imam Khomeini(RAH) Shahr-e-Rey Branch, Islamic Azad University, Tehran, Iran

[2]Department of Biology, Yadegar-e Imam Khomeini(RAH) Shahr-e-Rey Branch, Islamic Azad University, Tehran, Iran

[3]Department of Chemistry, Faculty of Pharmaceutical Chemistry, Tehran Medical Sciences, Islamic Azad University, Tehran, Iran

ARTICLE INFO

Article History:
Received 2022-01-20
Accepted 2022-07-25
Published 2022-12-22

Keywords:
Metal-organic framework,
Magnetic nanoparticles,
Drug delivery,
Release,
Capecitabine.

ABSTRACT

This study developed a novel silica-coated magnetic nanoparticle (Fe_3O_4@SiO_2@Cu BTC) based on a metal-organic framework (MOF) for targeted anticancer medication delivery. Using a co-precipitation method, the Fe_3O_4@SiO_2 core was coated with $Cu(OH)_2$ shell, which was then converted to CuBTC in a hydroethanolic mixture. Finally, a post-synthetic approach was used to manufacture a 3-(mercaptopropyl) trimethoxysilane functionalized Fe_3O_4@SiO_2@Cu BTC nanocomposite. The resulting material is characterized using SEM-EDX, TEM, VSM, XRD, TGA, BET, UV–Vis, and FT-IR techniques. TEM and SEM micrographs confirmed the core-shell structure. The resulting nanocomposite has high thermal stability, according to TGA findings. Because of their great biocompatibility and drug loading capability, coated Fe_3O_4@SiO_2@Cu BTC nanoparticles might be perfect for drug delivery. Capecitabine (CAP), an anticancer medication, was successfully dispersed through MOF pores. The acquired data revealed that 91 percent of the CAP was adsorbed on the constructed framework, and that the release of capecitabine in PBS buffer solution (pH 5.7) at 37 °C took up to 60 hours to complete. The findings show that nano-sized MOFs-based magnetic NPs with high drug loading and acceptable biocompatibility are viable options for targeted drug delivery.

How to cite this article
Asgari Pari A., Samadi S., Allahgholi Ghasri M. R., Bikhof Torbati M., Yousefi M., Preparation and Characterization of Silica Coated Magnetic Cu Based MOF as a Nanocarrier for Gradual Release of the Capecitabine Anticancer Drug. J. Nanoanalysis., 2022; 9(4): 283-293. DOI: 10.22034/jna.2022.1946948.1288

INTRODUCTION

Finding new and creative cancer treatments and carriers is a big challenge all around the globe [1]. Today, significant advances have been made in the treatment of various diseases by using modern techniques in drug delivery. New carriers including porous surface adsorbents and Metal Organic Frameworks (MOFs) have been widely studied and utilized for cancer treatment, and they play an important role as drug transporters [2]. Recent breakthroughs in MOF and nanoporous materials have aided in the treatment of cancer [3]. Micelles [4], liposomes [5], nanogels [6], mesoporous silica [7,8], dendrimers [9], polymeric nanoparticles [10,11], nanocatalyst [12-14], and magnetic nanoparticles [15] are only a few of the nanocarriers that have been used in cancer

* Corresponding Author Email: *myousefi50@hotmail.com*

treatment. Targeted drug delivery systems (DDS) or smart DDS has been used as a startling strategy in advanced cancer treatment throughout the past several decades [16-18]. The customizable size, high agent loading, biocompatibility, and ease of chemical functionalization of MOFs made of metal ions bridged by organic ligands have piqued interest [19]. MOFs have recieved a lot of attention from researchers and academics since Yaghi et al. initially used them in 1999 because of their large specific surface area, ultra-high porosity, high pore volume changeable pore size, and great chemical and thermal stability [20]. MOFs are extensively employed in a variety of domains, including gas storage [21], catalysis [22], sensors [23], and medicinal applications, including drug delivery [24].Magnetic metal-organic frameworks (MMOFs) have sparked a lot of attention in the last ten years since they have a lot of applications in biomedical chemistry [25]. When compared to other MOFs, MMOFs offer various benefits, including (I) precise selection of an appropriate target material, [26] (ii) simple separation from mixed solutions [27], (III) good dispersion, and (IV) many reuses are all advantages. The utilization of MMOFs for the targeted delivery of NPs to the place of interest with the guidance of an externally supplied magnetic field is enabled by the synergistic actions of MOFs and magnetic particles [28]. As a result, drug delivery applications are appealing to MMOF materials [29]. Because of the simplicity of functionalization, high stability, enhanced dispersibility, and resistance to degradation and agglomeration, silica coated magnetic MOFs are excellent alternatives for drug delivery [30]. Cu-MOFs, among the many types of MOFs, have shown to have a lot of promise and interesting applications in current material science [31]. Cu-MOFs are made up of oxygen, nitrogen, various organic ligands, and copper ions that form when the coordination polymer self-assembles. Due to its high solubility, trimesic acid (H_3BTC) was used as a linker precursor in many experiments to examine the production of MOFs. H_3BTC is a low-cost, rigid-structured tricarboxylic acid that has been utilized to make a variety of MOFs [32]. Capecitabine is one of the most significant cancer treatments, and it belongs to the antineoplastics (cancer therapies) class of chemicals [33]. Despite several investigations on magnetic MOFs as innovative drug delivery systems, there is still a need to develop new nanocarriers for capecitabine progressive release (CAP). There has been no report on the use of MOF as a nanocarrier for CAP loading and release to yet. MMOFs have been used to administer and release cancer medicines in a variety of ways. Fe_2O_3@MOFs were synthesized by Yi-nan Wu et al. for loading and releasing Ibuprofen [34]. Martin E et al. [35] produced a novel kind of magnetic NPs/MOF carriers that might be used in targeted medication delivery systems. In addition, the scientific group of Javanbakht et al. produced ibuprofen-loaded Cu-based MOFs and discovered that the medication was released within 24 hours [36]. Lin Hou et al. developed a Cu-based metal-organic framework-based antitumor efficacy triggering system (MOF). This approach offered a viable technique for using DSF in tumor treatment [37]. Also, a novel form of magnetic nanocarrier for DOX delivery and controlled release based on Fe_3O_4@PDA@ ZIF-90 [38]. Wu et al. used $Fe(acac)_3$@MIL-53(Al) pyrolysis to create Fe_2O_3@ MIL-53(Al). The ibuprofen loading in the prepared MOFs was reported to be about 9.9% and released for five days.We provide a unique strategy to constructing a simple and cost-effective tailored medicine delivery system based on MMOFs. By combining silica-coated Fe_3O_4 NPs with Cu -BTC (benzene-1,3,5-tricarboxylate) as an effective MOF, the Fe_3O_4/SiO_2/Cu BTC nanocomposite was created (Scheme 1). FT-IR, XRD, SEM, EDX, BET, and TEM methods were used to analyze the structural and morphological characteristics of the produced magnetic MOFs. The anticancer medication capecitabine (CAP) was used as a model to explore drug loading and release characteristics.

EXPERIMENTAL

Materials and methods

Ferrous chloride ($FeCl_2.4H_2O$), ferric chloride ($FeCl_3.6H_2O$), ethanol, ammonium

hydroxide ($NH_3.H_2O$), tetraethylorthosilicate (TEOS), copper chloride ($CuCl_2 \cdot H_2O$), trimesic acid (H_3BTC), toluene(anhydrous), (3-mercaptopropyl)trimethoxysilane, were bought from Merck Company, Germany. The active ingredient of the capecitabine was provided from Temad Pharmaceutical Company, Iran. All chemicals and materials were utilized without purification procedures.

Synthesis of Fe_3O_4@SiO_2

Magnetic iron oxide nanoparticles were produced utilizing a co-precipitation method [39].

To begin, deionized water was used to dissolve $FeCl_3.6H_2O$ (2.307 g) and $FeCl_2.4H_2O$ (3.97 g) (100 mL). The mixture was then progressively added to diluted NH_3 solution (7.47 mL) under a N_2 atmosphere at 85 °C for two hours. The resulting black participant was combined with ethanol (80 mL), 40 mL of TEOS, and 2 mL of a diluted NH_3 solution at pH=11-12 for 16 hours with vigorous stirring. Finally, the product was collected using a powerful magnet, rinsed with a 1:1 (V/V) ethanol and water solution, and dried for 24 hours under vacuum at 80 °C.

Synthesis of $Fe_3O_4@SiO_2@Cu(OH)_2$

The $Fe_3O_4@SiO_2@Cu(OH)_2$ MNPs were synthesized using the previously described co-precipitation technique. In 200 mL DI H_2O containing 1.0 g $CuCl_2 \bullet H_2O$, 0.5 g $Fe_3O_4@SiO_2$ was added. The resulting product was then ultrasonically mixed for 20 minutes, and the pH was corrected to 9.0-10.0 by stirring in NaOH solution. For three hours, the mixture was held at 85°C. Finally, the product was washed in deionized water and ethanol before being vacuum dried at 50°C for 24 hours [40].

Synthesis of $Fe_3O_4@SiO_2@CuBTC$

The $Fe_3O_4@SiO_2@Cu$ -BTC composite was made using the method described in ref [41] with minor changes. 0.440 g of $Fe_3O_4@SiO_2@Cu(OH)_2$ was disseminated in for deionized water this purpose (8Ml). The solution was then treated with 16 mL of ethanol solution containing 0.063 g H3BTC to convert Cu(OH)2 to Cu -BTC. The mixture was rapidly agitated at room temperature for 12 hours, and the required result was separated, washed multiple times with deionized water and dried for 12 hours at 150 degrees Celsius.

Mercapto-functionalization of $Fe_3O_4@SiO_2@CuBTC$

$Fe_3O_4@SiO_2@$ CuBTC MNPs (2g) was added to the solution of 47.5 ml of anhydrous

toluene and 23.5 ml of 3-(mercaptopropyl) trimethoxysilane, and then refluxed under vigorous

stirring for 20 h. The modified magnetic nanoparticles were washed with toluene and dried at 60˚C for 12 h. [42].

Synthesis of powder nano-capsules

0.2 g of synthesis magnetic nanoparticles and 0.1 g of capecitabine were dispersed into 150 mL of deionized water and stirred at 90˚C for five h. After that, the product was centrifuged, rinsed with water and dried at 80 ˚C [43].

Drug release

In order to release capecitabine in a malignant cell and a healthy human body state (pH 5.7 and 7.4) in an in-vitro environment, the simulated circumstances need first be created in the laboratory. At 37 degrees Celsius, 0.2 grams of powdered nano-capsule containing $Fe_3O_4@SiO_2@$ CuBTC@CAP was distributed in 40 milliliters of water and three drops of phosphate buffer saline (pH 5.7 and 7.4). After that, samples were obtained at various periods between 0 and 60 hours to capture UV-Vis data.

Characterization

The functional group of the collected samples was determined using a Bruker Fourier transforms infrared spectrometer (FT-IR) (Thane, Maharashtra, India). An X-ray diffractometer was used to conduct the XRD study (PANalytical, Philips, the Netherlands). A Rheumatic Scientific TG/DTA STA 1500 (USA) with a heating rate of 10 Cmin-1 was used for thermodynamic analysis (TGA). Emission from the field for surface morphology and particle size assessment on as-prepared materials, scanning electron microscopy (FESEM) (model TESCAN Mira3, Czech Republic, and model SIGMA VP, ZEISS Company, Germany) was applied. BET was used to determine the surface area and pore volume of the produced materials using an ASAP 2020 equipment (Micromeritics, USA) and N_2 as an inert gas. A vibrating sample magnetometer was used to assess the items magnetic properties (VSM). A spectrophotometer was used to determine the concentration of capecitabine (Perkin Elmer UV-Vis spectrophotometer, Lambda 25, USA).

RESULTS AND DISCUSSION

Sample characterizations

Fourier-transform infrared spectroscopy

FT-IR spectra of $Fe_3O_4@SiO_2$, $Fe_3O_4@SiO_2@Cu(OH)_2$, $Fe_3O_4@SiO_2@Cu$ BTC and mercapto modified $Fe_3O_4@SiO_2@Cu$ BTC are indicated in Fig. 1. In the FT-IR spectra of $Fe_3O_4@SiO_2$, a wide peak around 1090 cm^{-1} was observed, which was attributed to the stretching vibration of O-Si-O, showing the successful preparation of $Fe_3O_4@SiO_2$. As illustrated in Fig 1(b), the absorption bands at 600 cm^{-1} and 1000 cm^{-1} were attributed to Cu-O vibrations, Cu-OH and OH stretching vibrations,

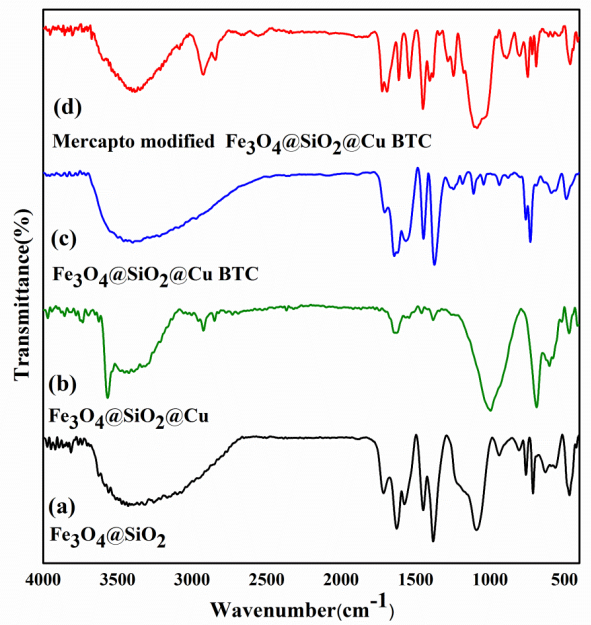

Fig. 1. FT-IR spectra of (a):Fe_3O_4@ SiO_2, (b):Fe_3O_4@SiO_2@ $Cu(OH)_2$, (c) Fe_3O_4@SiO_2@ Cu BTC, (d) mercapto modified Fe_3O_4@SiO_2@ Cu BTC

which proved that $Cu(OH)_2$ was successfully immobilized on the surface of magnetic Fe_3O_4@ SiO_2 nanoparticles.

The OH group of surface adsorbed water molecules was ascribed to the broadband at 3398 cm^{-1} for Fe_3O_4@SiO_2@Cu BTC, as were absorption peaks of the C=O bonds (1642 cm^{-1} and 1564 cm^{-1}) and stretching, vibration absorption peaks of C=C bonds on the benzene ring (1446 cm^{-1} and 1373 cm^{-1}). Fig. 1(b) demonstrated that the absorption bands at 729 and 487 cm^{-1} in Cu-BTC and iron oxide, respectively, were connected with Cu-O and Fe-O-Fe bonds. The aliphatic S-H stretch vibrations of the mercapto agent resulted in a large absorption band of around 2900 cm^{-1} in the spectra of 1(C).

X-ray Diffractions

Fig. 2 shows the XRD patterns of (a) Fe_3O_4@SiO_2, (b) Fe_3O_4@SiO_2@Cu BTC and mercapto modified Fe_3O_4@SiO_2@Cu BTC (c), respectively. In (a), the diffraction peaks at 2θ= 30.01˚, 36.01˚, 43.02˚, 53.61˚, 57.11˚and 62.81˚ are related to (220), (311), (422), (400), (511) and (540) Bragg reflections, respectively, which accorded well with the standard cubic spinel structure of Fe_3O_4 (reference JCPDS cad no. 19-629). Additionally, several peaks are presented at diffraction angles at 2θ= 10-20˚, which could be attributed to the amorphous phase of SiO_2. Moreover, the diffraction peaks of Fe_3O_4@SiO_2@ Cu BTC were in accordance with the published literature [44]. The major peaks of the mercapto-modified Fe_3O_4@SiO_2@CuBTC composite were consistent with Fe_3O_4@SiO_2@Cu BTC. Thus, the intensity of characteristic diffraction peaks was gradually reduced in terms of the encapsulation of Cu-BTC and surface modification of Fe_3O_4@SiO_2@ Cu BTC with the mercapto functional group.

Furthermore, the FullProf program examined all of the collected XRD patterns using the Rietveld refinement technique. The Rietveld method is often used to extract structural information from XRD data. This approach compares Bragg parameters to those generated from a hypothetical structural model using a least-squares fitting formula. Furthermore, the Rietveld factors are calculated to assess the fitting elements of the experimental data, including the goodness of fit (2) and various R factors (RF = crystallographic factor and RWP=weighted profile R-value). The best fitting quality to the experimental XRD data is attained when the aforementioned parameters reach their optimal value, and the crystal structure is regarded acceptable. Table 1 shows the Rietveld refined data collected for all produced samples. The low value of 2 achieved for all synthesized materials demonstrated the Rietveld refinement suitability. Crystallite sizes calculated from the Rietveld method are listed in Table 1. We have

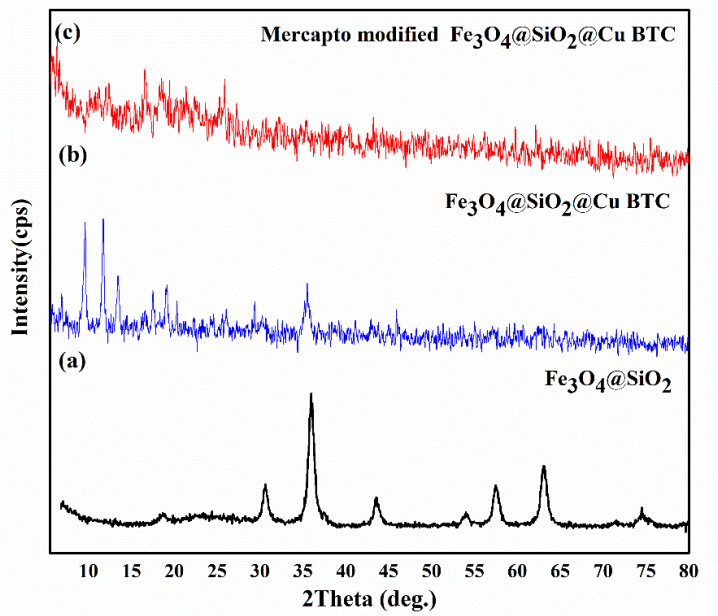

Fig. 2. XRD patterns of (a) Fe_3O_4@SiO_2, (b) Fe_3O_4@SiO_2@Cu BTC and (c) mercapto modified Fe_3O_4@SiO_2@Cu BTC

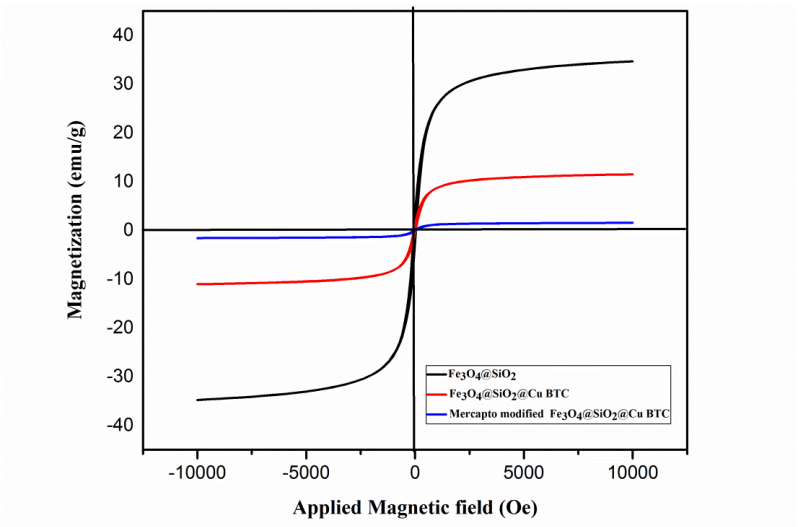

Fig. 3. Magnetization curves of (a) Fe_3O_4@SiO_2, (b) Fe_3O_4@SiO_2@Cu BTC nanocomposite and (c) mercapto modified Fe_3O_4@SiO_2@ Cu BTC

observed that the crystallite sizes of Fe_3O_4 and SiO_2 in both the Fe_3O_4@SiO_2 and Fe_3O_4@SiO_2@Cu BTC samples were increased. According to Table 1, it can be observed that the crystallite size of mercapto modified Fe_3O_4@SiO_2@Cu BTC nanocomposites was reduced after surface modification. This phenomenon can be due to the compaction of crystal structure after surface modification of Fe_3O_4@SiO_2@Cu BTC with mercapto groups. The mercapto modified nanocomposite indicated the lowest Cu-BTC weight percentage, suggesting hydrolysis or decomposition of the materials during the drying process, which is observable in the TGA data.

Magnetic properties of the prepared samples

VSM was used to test the magnetic behavior of the as-prepared nanomaterials at room temperature. The VSM curves of Fe_3O_4@SiO_2 (a), Fe_3O_4@ SiO_2@ CuBTC (b), and mercapto modified nanocomposite

Table 1. Crystallite sizes of samples by Rietveld method

Samples	Fe_3O_4			SiO_2			Cu-BTC			Fit Parameters	
	Percent (%)	Crystallite Size (Å)	Cell Parameter (Å)	Percent (%)	Crystallite Size (Å)	Cell Parameter (Å)	Percent (%)	Crystallite Size (Å)	Cell Parameter (Å)	χ^2	Rwp
Fe_3O_4@SiO_2	96.958	1710.554	a= 8.4026	3.042	270.559	a= 6.4586	-	-	-	1.92	15.0
Fe_3O_4@SiO_2@Cu BTC	56.886	1940.7	a= 8.4267	3.4899	280.4267	a= 6.457	39.62	212.4	a= 26.5155	1.97	9.17
Mercapto modified nanocomposite	66.54	1780.0	a= 8.427	6.270	168.0	a= 6.4616	27.1891	193.8	a= 26.6018	1.98	9.68

Table 2. BET specific surface area and pore volumes of the obtained samples

Material	BET surface area (m^2g^{-1})	Pore volume
Fe_3O_4 @SiO_2	29.81	0.04
Fe_3O_4 @SiO_2@ $Cu(OH)_2$	45.60	0.26
Fe_3O_4 @SiO_2@Cu-BTC	152.87	0.49
Mercapto modified Fe_3O_4 @SiO_2@Cu-BTC	78.36	0.29

(c) are shown in Fig. 3. (c). As shown in Fig. 3, all produced samples exhibited a superparamagnetic behavior, and the saturation magnetization (Ms) clearly decreased with the addition of CuBTC species. Due to the encapsulation of CuBTC on silica-coated Fe_3O_3 NPs surface, the Ms value of Fe_3O_4@ SiO_2@CuBTC nanocomposite (34.96 emu g^{-1}) was much lower than Fe_3O_4@ SiO_2 (11.55 emu g^{-1}). An external magnetic field may also be used to recover the Fe_3O_4@ SiO_2@CuBTC nanocomposite from a solution, as demonstrated in Fig. 3.

Nitrogen adsorption/ desorption of the prepared samples

The surface and pore structure of the as-synthesized magnetic nanocomposites were further assessed by nitrogen adsorption/desorption analysis (BET), with the findings shown in Table 2. Fe_3O_4 @ SiO_2 had a surface area (SBET) of 29. 81 m^2g^{-1} and a total pore volume (Vm) of 0.04 $cm^3 g^{-1}$, according to the data. Meanwhile, after encapsulating Cu-BTC, SBET and Vm were enhanced to 152.87 m^2g^{-1} and 0.2908 cm^3 g^{-1}, respectively, indicating that $Cu(OH)_2$ was successfully converted to Cu-BTC. The BET surface area of Fe_3O_4 @SiO_2 @Cu-BTC was significantly reduced following surface modification with the mercapto functional group, as shown in Table 1. Mercapto modified Fe_3O_4 @ SiO_2@ Cu-BTC surface area decreased dramatically from 152.87 m^2g^{-1} to 78.36 m^2g^{-1}.

Evaluation of SEM-EDX

Scanning electron microscopy was used to examine the structural and morphological

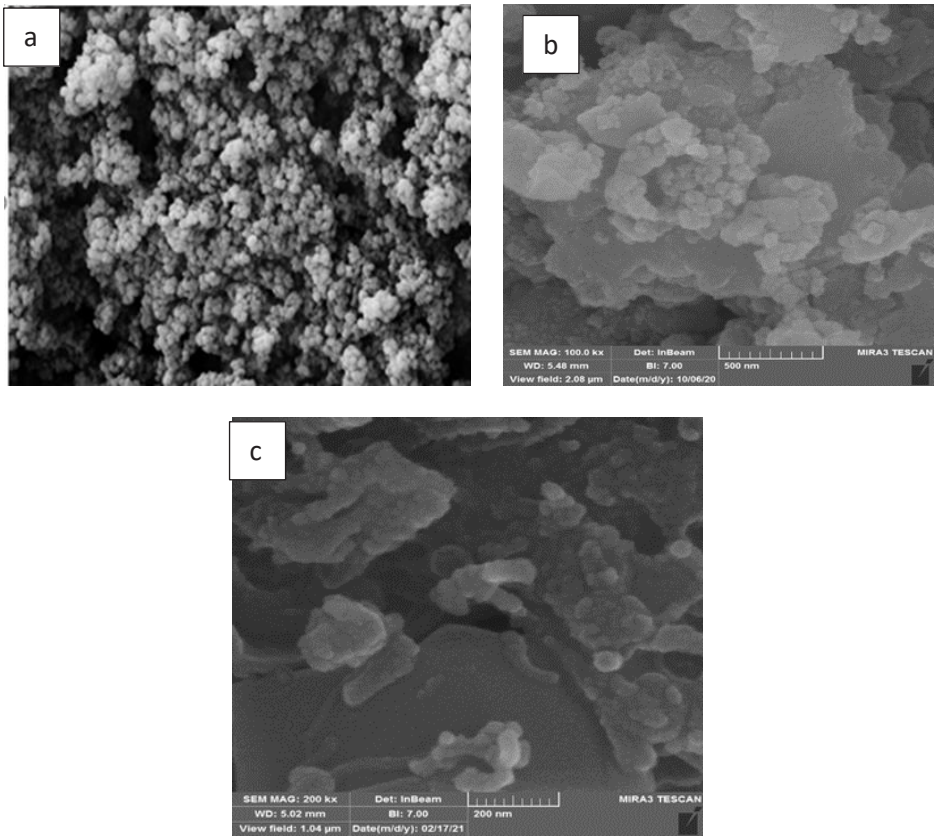

Fig. 4. SEM micrographs of (a) Fe_3O_4@SiO_2, (b) Fe_3O_4@SiO_2@CuBTC and (c) mercapto modified Fe_3O_4@SiO_2@CuBTC nanocomposites

properties of (a) Fe_3O_4 @SiO_2 and (b) Fe_3O_4@SiO_2 @CuBTC nanocomposites, as well as mercapto modified Fe_3O_4@SiO_2@Cu-BTC nanocomposites. Fe_3O_4@SiO_2 NPs were spherical with an average diameter of 40 nm, as shown in Fig 4(a). The diameter was raised to 70 nm after being encased with Cu-BTC MOF (Fig. 4b). Fe_3O_4@SiO_2@Cu-BTC shape was discovered as a regular core-shell-like structure. Cu-BTC seems to have magnetized and agglomerated tiny particles of magnetic NPs. Fig. 4 shows the related energy-dispersive X-ray (EDX) spectra in order to determine the chemical structure of the mercapto modified Fe_3O_4@SiO_2@ Cu BTC nanocomposite. The existence of Fe, Si, S, Cu, C, and O components in the chemical composition of the final magnetic mercapto modified nanocomposite is shown by the EDX spectrum.

A transmission electron microscopy (TEM) picture of magnetic Fe_3O_4@SiO_2@Cu-BTC nanocomposite is displayed in Fig. 6 to further analyze particle shape and size distribution. The produced Fe_3O_4@SiO_2@Cu-BTC product had a semi-spherical form, and the surface topography of the core-shell-like nanocomposite was rough, as shown in Fig.6. Due to the strong electrostatic interactions between Fe_3O_4@SiO_2 and Cu-BTC motifs, a relative agglomeration was also observed. Furthermore, after being encapsulated with Cu-BTC, the size of Fe_3O_4 NPs increased.

Thermogravimetric analysis of the prepared sample

TGA was used to evaluate the magnetic Fe_3O_4@ SiO_2@Cu-BTC nanocomposite thermal behavior and stability. The initial weight loss (13%) is due to moisture evaporation in the micropores of the obtained sample, as seen in Fig. 7. When the Cu-BTC complex collapses, the second weight loss (300 to 450 °C) occurs. From the standpoint of thermal stability, the ultimate weight loss (450-550) shows the disintegration of mercapto species; this magnetic nanocomposite is ideal for cancer therapy.

Sustained drug release

The use of magnetic Fe_3O_4@SiO_2@Cu-BTC as a

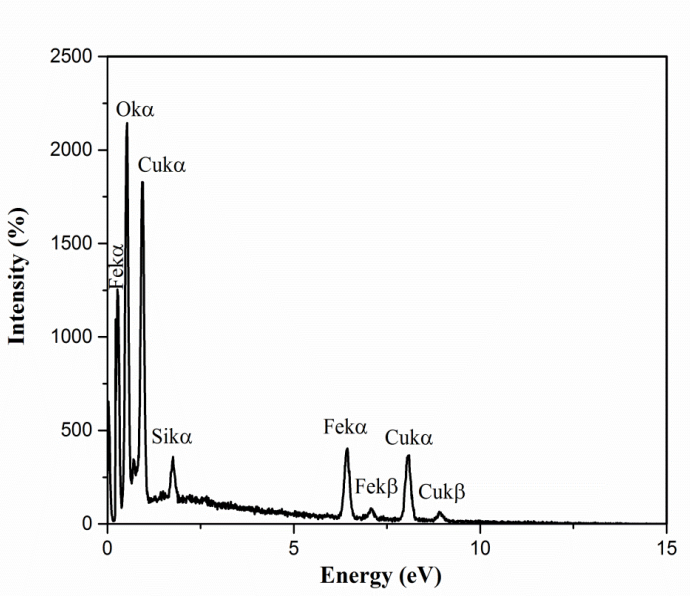

Fig. 5. EDX spectrum of mercapto modified Fe_3O_4@SiO_2@Cu-BTC

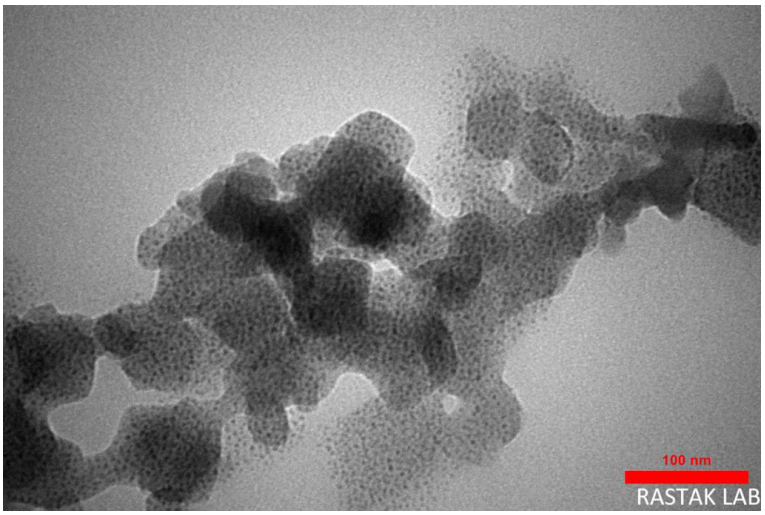

Fig.6. TEM image of Fe_3O_4@SiO_2@Cu-BTC sample

targeted drug delivery device was examined. This material was chosen because of its biocompatibility and large surface area. The ability of mercapto modified Fe_3O_4@SiO_2@Cu-BTC as a pH-responsive nanocarrier was evaluated using capecitabine as a biological model. Anticancer medication formulations need controlled drug release. The release profile of CAP was investigated using a PBS buffer solution with pH values of 5.7 and 7.4. To model drug release behavior in the malignant cell surrounding environment, Fig. 8 shows the release of CAP from Fe_3O_4@SiO_2@Cu-BTC/ CAP nanocapsule in acidic and neutral media. The produced nanocarrier displays regulated CAP release properties in PBS solution, as predicted, because to the comparatively high loading efficiency of Fe_3O_4@SiO_2@Cu-BTC. The total CAP release from Fe_3O_4@SiO_2@Cu-BTC was reached after 60 h in PBS buffer at pH 5.7, as shown by the time-dependent release curve (Fig. 8). Because of the physical sorption of CAP on the magnetic nanocarrier, around 40% of the CP were released over the first seven hours, according to the release profile. Following that, CAP release increased steadily, with 45 percent released within 15 hours due to anticancer drug diffusion from Cu-BTC pores into the PBS solution. This may be attributed to the strong interaction between the Fe core and

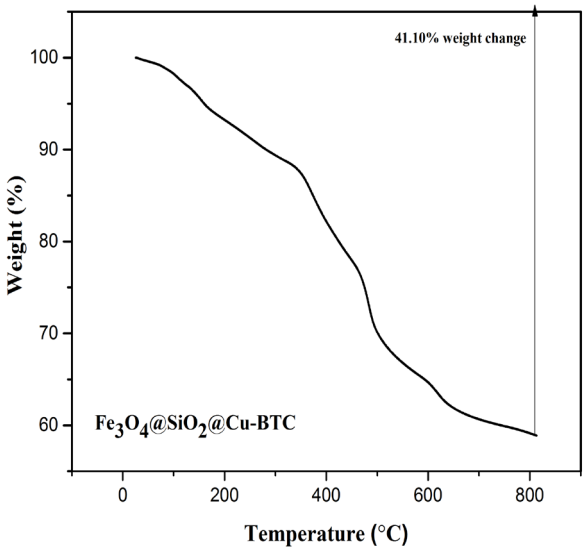

Fig. 7. Thermogravimetric analysis of Fe_3O_4@SiO_2@Cu-BTC sample

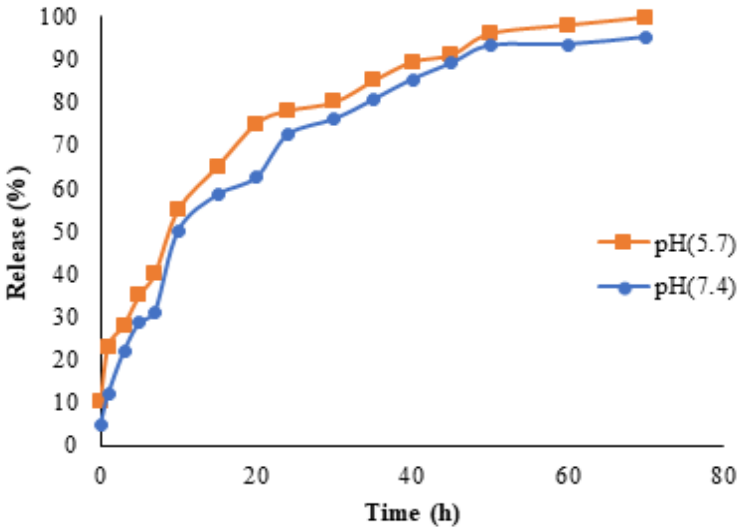

Fig. 8. The CAP release profile from Fe_3O_4@SiO_2@Cu-BTC nanocarrier in PBS solution at pHs 5.7 and 7.4.

base groups of CAP drug molecules, since the final loaded medication (approximately 12 percent) was released for up to 40 hours. Only 72 percent loaded capecitabine in mercapto modified Fe_3O_4@SiO_2@Cu-BTC released in PBS at pH 7.4 during 24 hours.The findings showed that the mercapto modified Fe_3O_4@SiO_2@Cu-BTC nanocomposite, as synthesized, provides a viable platform for targeted anticancer drug delivery as a new nanocarrier.

CONCLUSIONS

We created a Cu-BTC motif on the surface of nano-sized core-shell magnetic NPs (Fe_3O_4@SiO_2@Cu-BTC) as a nanocarrier for regulated drug administration of CAP, and FT-IR, SEM, TEM, XRD, and BET analytical techniques were used to determine its structural characteristics. The core-shell shape of the produced Fe_3O_4@SiO_2@Cu-BTC was validated by SEM and TEM analysis, and the superparamagnetic behavior of the magnetic nanocomposite was shown using the VSM method. The magnetic iron oxide core gave the nanocarrier a strong magnetic property, allowing for controlled drug release and simple removal. In

mercapto modified Fe_3O_4@SiO_2@Cu-BTC released within 24 hours in PBS at pH 7.4, Fe_3O_4@SiO_2@Cu-BTC nanoparticles with a mean size of 70 nm can load CAP antitumor drug and 72 percent loaded capecitabine in Fe_3O_4@SiO_2@Cu-BTC nanoparticles with a mean size of 70 nm can load CAP antitumor. As a result, the created MMOFs networks were shown to be successful in controlling the release of anticancer drugs. In addition, further in-vivo tests are needed to examine the magnetic drug delivery system enormous potential as a theranostic platform for the treatment of various malignancies.

ACKNOWLEDGEMENTS

The authors are humbly thankful to Yadegar-e Imam Khomeini(RAH) Shahr-e Rey and Tehran Medical Sciences Branch, Islamic Azad University, for supporting this study.

CONFLICT OF INTEREST

The authors declare no conflicts of interest.

REFERENCES

[1] Mateo J, Steuten L, Aftimos P, André F, Davies M, Garralda E, Geissler J, Husereau D, Martinez-Lopez I, Normanno N, Reis-Filho JS. Delivering precision oncology to patients with cancer. Nature Medicine. 2022;28(4):658-65. https://doi.org/10.1038/s41591-022-01717-2

[2] Zeng Y, Zhang C, Du D, Li Y, Sun L, Han Y, He X, Dai J, Shi L. Metal-organic framework-based hydrogel with structurally dynamic properties as a stimuli-responsive localized drug delivery system for cancer therapy. Acta Biomaterialia. 2022;145:43-51. https://doi.org/10.1016/j.actbio.2022.04.003

[3] Lucky SS, Soo KC, Zhang Y. Nanoparticles in photodynamic therapy. Chemical reviews. 2015;115(4):1990-2042. https://doi.org/10.1021/cr5004198

[4] Deng C, Jiang Y, Cheng R, Meng F, Zhong Z. Biodegradable polymeric micelles for targeted and controlled anticancer drug delivery: promises, progress and prospects. Nano Today. 2012;7(5):467-80. https://doi.org/10.1016/j.nantod.2012.08.005

[5] Cheung C, Al-Jamal WT. Liposomes-based nanoparticles for cancer therapy and bioimaging, in Nanooncology. 2018; Springer:51-87. https://doi.org/10.1007/978-3-319-89878-0_2

[6] Molina M, Asadian-Birjand M, Balach J, Bergueiro J, Miceli E, Calderón M. Stimuli-responsive nanogel composites and their application in nanomedicine. Chemical Society Reviews. 2015;44(17):6161-86. https://doi.org/10.1039/C5CS00199D

[7] He Q, Shi J. Mesoporous silica nanoparticle based nano drug delivery systems: synthesis, controlled drug release and delivery, pharmacokinetics and biocompatibility. Journal of Materials Chemistry. 2011;21(16):5845-55. https://doi.org/10.1039/c0jm03851b

[8] Saghi M, Shokri A, Arastehnodeh A, Khazaeinejad M, Nozari A The photo degradation of methyl red in aqueous solutions by α-Fe2O3/SiO2 nano photocatalyst. Journal of Nanoanalysis. 2018;5(3):163-70.

[9] Fu F, Wu Y, Zhu J, Wen S, Shen M, Shi X. Multifunctional lactobionic acid-modified dendrimers for targeted drug delivery to liver cancer cells: investigating the role played by PEG spacer. ACS Applied Materials & Interfaces. 2014;6(18):16416-25. https://doi.org/10.1021/am504849x

[10] Guo Y, Chu M, Tan S, Zhao S, Liu H, Otieno BO, Yang X, Xu C, Zhang Z. Chitosan-g-TPGS nanoparticles for anticancer drug delivery and overcoming multidrug resistance. Molecular pharmaceutics. 2014;11(1):59-70. https://doi.org/10.1021/mp400514t

[11] Rostami M, Mazaheri H, Hassani Joshaghani A, Shokri A. Usingexperimentaldesigntooptimizethephoto-degradation of P-nitro toluene by Nano-TiO2 in synthetic wastewater. International Journal of Engineering. 2019;32(8):1074-81. https://doi.org/10.5829/ije.2019.32.08b.03

[12] Shokri A. Using Mn based on lightweight expanded clay aggregate (LECA) as an original catalyst for the removal of NO2 pollutant in aqueous environment. Surfaces and Interfaces. 2020;21:100705. https://doi.org/10.1016/j.surfin.2020.100705

[13] Rostami M, Hassani Joshaghani A, Mazaheri H, Shokri A. Photo-degradation of P-Nitro Toluene Using Modified Bentonite Based Nano-TiO2 Photocatalyst in Aqueous Solution. International Journal of Engineering. 2021;34(4):756-62. https://doi.org/10.5829/ije.2021.34.04a.01

[14] Shokri A. Using NiFe2O4 as a nano photocatalyst for degradation of polyvinyl alcohol in synthetic wastewater. Environmental Challenges. 2021;5:100332. https://doi.org/10.1016/j.envc.2021.100332

[15] Dhavale RP, Dhavale RP, Sahoo SC, Kollu P, Jadhav SU, Patil PS, Dongale TD, Chougale AD, Patil PB. Chitosan coated magnetic nanoparticles as carriers of anticancer drug Telmisartan: pH-responsive controlled drug release and cytotoxicity studies. Journal of Physics and Chemistry of Solids. 2021;148:109749. https://doi.org/10.1016/j.jpcs.2020.109749

[16] Chowdhuri AR, Bhattacharya D, Sahu SK. Magnetic nanoscale metal organic frameworks for potential targeted anticancer drug delivery, imaging and as an MRI contrast agent. Dalton Transactions. 2016;45(7):2963-73. https://doi.org/10.1039/C5DT03736K

[17] Yousefi M, Safari M, Torbati MB, Kazemiha VM, Sanati H, Amanzadeh A. New mononuclear diorganotin (IV) dithiocarboxylates: synthesis, characterization and study of their cytotoxic activities. Applied Organometallic Chemistry. 2012;26(8):438-44. https://doi.org/10.1002/aoc.2885

[18] Bikhof Torbati M, Ebrahimian M, Yousefi M, Shaabanzadeh M. GO-PEG as a drug nanocarrier and its antiproliferative effect on human cervical cancer cell line. Artificial cells, Nanomedicine, and Biotechnology. 2017;45(3):568-73. https://doi.org/10.3109/21691401.2016.1161641

[19] Liu J, Huang J, Zhang L, Lei J. Multifunctional metal-organic framework heterostructures for enhanced cancer therapy. Chemical Society Reviews. 2021;50(2):1188-218. https://doi.org/10.1039/D0CS00178C

[20] Wo R, Li QL, Zhu C, Zhang Y, Qiao GF, Lei KY, Du P, Jiang W. Preparation and characterization of functionalized

metal-organic frameworks with core/shell magnetic particles (Fe3O4@ SiO2@ MOFs) for removal of Congo red and methylene blue from water solution. Journal of Chemical & Engineering Data. 2019;64(6):2455-63. https://doi.org/10.1021/acs.jced.8b01251

[21] Boukoussa B, Abidallah F, Abid Z, Talha Z, Taybi N, El Hadj HS. Synthesis of polypyrrole/Fe-kanemite nanocomposite through in situ polymerization: effect of iron exchange, acid treatment, and CO2 adsorption properties. Journal of Materials Science. 2017;52(5):2460-72. https://doi.org/10.1007/s10853-016-0541-0

[22] Kaur R, Vellingiri K, Kim K-H, Paul A, Deep A. Efficient photocatalytic degradation of rhodamine 6G with a quantum dot-metal organic framework nanocomposite. Chemosphere. 2016;154:620-7. https://doi.org/10.1016/j.chemosphere.2016.04.024

[23] Qi Z, Chen Y. Charge-transfer-based terbium MOF nanoparticles as fluorescent pH sensor for extreme acidity. Biosensors and Bioelectronics. 2017;87:236-41. https://doi.org/10.1016/j.bios.2016.08.052

[24] Ma R, Yang P, Ma Y, Bian F. Facile Synthesis of Magnetic Hierarchical Core-Shell Structured Fe3O4@ PDA-Pd@ MOF Nanocomposites: Highly Integrated Multifunctional Catalysts. ChemCatChem. 2018;10(6):1446-54. https://doi.org/10.1002/cctc.201701693

[25] Ricco R, Malfatti L, Takahashi M, Hill AJ, Falcaro P. Applications of magnetic metal-organic framework composites. Journal of Materials Chemistry A. 2013;1(42):13033-45. https://doi.org/10.1039/c3ta13140h

[26] Maya F, Cabello CP, Frizzarin RM, Estela JM, Palomino GT, Cerdà V. Magnetic solid-phase extraction using metal-organic frameworks (MOFs) and their derived carbons. TrAC Trends in Analytical Chemistry. 2017;90:142-52. https://doi.org/10.1016/j.trac.2017.03.004

[27] Zhao X, Liu S, Tang Z, Niu H, Cai Y, Meng W. Synthesis of magnetic metal-organic framework (MOF) for efficient removal of organic dyes from water. Scientific Reports. 2015;5(1):1-10. https://doi.org/10.1038/srep11849

[28] Simon-Yarza T, Giménez-Marqués M, Mrimi R, Mielcarek A, Gref R, Horcajada P. A smart metal-organic framework nanomaterial for lung targeting. Angewandte Chemie. 2017;129(49):15771-75. https://doi.org/10.1002/ange.201707346

[29] Osterrieth JW, Fairen-Jimenez D. Metal-organic framework composites for theragnostics and drug delivery applications. Biotechnology Journal. 2021;16(2):2000005. https://doi.org/10.1002/biot.202000005

[30] Wang X, Liang T, Zheng Z, Guo R, Zhang Z. MOF-silica hybrid derived high performance K-Cu# SiO2 catalyst for furfural valorization: the functional role of potassium acetate (KAc) in hybridization and copper electronic state. Applied Catalysis A: General. 2022:118603. https://doi.org/10.1016/j.apcata.2022.118603

[31] Li L, Liu XL, Gao M, Hong W, Liu GZ, Fan L. The adsorption on magnetic hybrid Fe3O4/HKUST-1/GO of methylene blue from water solution. Journal of Materials Chemistry A. 2014;2(6):1795-801. https://doi.org/10.1039/C3TA14225F

[32] Sanchez-Sala M, Vallcorba O, Domingo C, Ayllón JA. Acetic acid as a solvent for the synthesis of metal-organic frameworks based on trimesic acid. Polyhedron. 2019;170:458-62. https://doi.org/10.1016/j.poly.2019.06.017

[33] Anand U, Dey A, Chandel AK, Sanyal R, Mishra A, Pandey DK, De Falco V, Upadhyay A, Kandimalla R, Chaudhary A, Dhanjal JK. Cancer chemotherapy and beyond: Current status, drug candidates, associated risks and progress in targeted therapeutics. Genes & Diseases (2022), (in press). https://doi.org/10.1016/j.gendis.2022.02.007

[34] Wu Yn, Zhou M, Li S, Li Z, Li J, Wu B. Magnetic metal-organic frameworks: γ-Fe2O3@ MOFs via confined in situ pyrolysis method for drug delivery. Small. 2014;10(14):2927-36. https://doi.org/10.1002/smll.201400362

[35] Silvestre ME, Franzreb M, Weidler PG, Shekhah O, Wöll C. Magnetic Cores with Porous Coatings: Growth of Metal-Organic Frameworks on Particles Using Liquid Phase Epitaxy. Advanced Functional Materials. 2013;23(9):1210-13. https://doi.org/10.1002/adfm.201370043

[36] Javanbakht S, Nezhad-Mokhtari P, Shaabani A, Arsalani N, Ghorbani M. Incorporating Cu-based metal-organic framework/drug nanohybrids into gelatin microsphere for ibuprofen oral delivery. Materials Science and Engineering: C. 2019;96:302-9. https://doi.org/10.1016/j.msec.2018.11.028

[37] Hou L, Liu Y, Liu W, Balash M, Zhang H. In situ triggering antitumor efficacy of alcohol-abuse drug disulfiram through Cu-based metal-organic framework nanoparticles. Acta Pharmaceutica Sinica B. 2021;11(7):2016-30. https://doi.org/10.1016/j.apsb.2021.01.013

[38] Chen J, Liu J, Hu Y, Tian Z, Zhu Y. Metal-organic framework-coated magnetite nanoparticles for synergistic magnetic hyperthermia and chemotherapy with pH-triggered drug release. Science and technology of advanced materials. 2019;20(1):1043-54. https://doi.org/10.1080/14686996.2019.1682467

[39] Morovati A, Panahi HA, Yazdani F. Grafting of allylimidazole and n-vinylcaprolactam as a thermosensitive polymer onto magnetic nano-particles for the extraction and determination of celecoxib in biological samples. International Journal of Pharmaceutics. 2016;513(1-2):62-7. https://doi.org/10.1016/j.ijpharm.2016.09.006

[40] Huang L, He M, Chen B, Hu B. A designable magnetic MOF composite and facile coordination-based post-synthetic strategy for the enhanced removal of Hg 2+ from water. Journal of Materials Chemistry A. 2015;3(21):11587-95. https://doi.org/10.1039/C5TA01484K

[41] Majano G, Pérez-Ramírez J. Scalable room-temperature conversion of copper (II) hydroxide into HKUST-1 (Cu3(btc)2). Advanced Materials. 2013;25(7):1052-7. https://doi.org/10.1002/adma.201370041

[42] Lajevardi A, Sadr MH, Yaraki MT, Badiei A, Armaghan M. A pH-responsive and magnetic Fe3O4@ silica@ MIL-100 (Fe)/β-CD nanocomposite as a drug nanocarrier: loading and release study of cephalexin. New Journal of Chemistry. 2018;42(12):9690-701. https://doi.org/10.1039/C8NJ01375F

[43] Kavousi F, Goodarzi M, Ghanbari D, Hedayati K. Synthesis and characterization of a magnetic polymer nanocomposite for the release of metoprolol and aspirin. Journal of Molecular Structure. 2019;1183:324-30. https://doi.org/10.1016/j.molstruc.2019.02.003

[44] Chowdhury P, Bikkina C, Meister D, Dreisbach F, Gumma S. Comparison of adsorption isotherms on Cu-BTC metal organic frameworks synthesized from different routes. Microporous and Mesoporous Materials. 2009;117(1-2):406-413. https://doi.org/10.1016/j.micromeso.2008.07.029